

Luminescent properties of $\text{Eu}(\text{tfa})_3$ complexes incorporated into MSU-4 mesoporous silica matrices

Lucas Falquetti Saliba^{1, §}, Paulo César de Sousa Filho¹, Gustavo Rocha de Castro², Osvaldo Antonio Serra¹, Marco Antonio Utrera Martines^{3, *}

¹ Rare Earth Laboratory – Chemistry Department FFCLRP-USP, São Paulo University, Av. Bandeirantes, 3900 - CEP 14040-901 - Ribeirão Preto - SP - Brazil

² Institute of Biosciences of Botucatu Sao Paulo State University, UNESP, PO Box 510, CEP 18618-000, Botucatu, SP, Brazil

³ Institute of Chemistry, Federal University of Mato Grosso do Sul, UFMS, CEP 79074-460, Campo Grande, MS, Brazil

§ *in memoriam*: Lucas Falquetti Saliba

*corresponding author e-mail address: marco.martines@ufms.br

ABSTRACT

A luminescent material has been prepared through formation of the Eu^{3+} β -diketonate complex $[\text{Eu}(\text{tfa})_3(\text{H}_2\text{O})_2]$ in methanolic medium within the channels of MSU-4 ordered mesoporous silica by post-grafting synthesis. Using simple wet incorporation methods, the Eu^{3+} ions were first impregnated into the solids, which was followed by addition of the 2-thenoyltrifluoroacetate (tfa) ligand. For further comparison, an analogous sample of the functionalized silica was impregnated with the previously prepared $[\text{Eu}(\text{tfa})_3(\text{H}_2\text{O})_2]$ complex. The materials were characterized by scanning and transmission electron microscopy (SEM/TEM), X-ray diffractometry (XRD), infrared spectroscopy (IR) and photoluminescence spectroscopy (PL). The photoluminescence studies at room temperature showed the characteristic absorption of the ligand in the ultraviolet range in the excitation spectra and remarkable differences were observed between the free and the immobilized complexes. The emission spectra displayed the typical Eu^{3+} intraconfigurational $^4\text{f}_6$ lines, ascribed to transitions between the $^5\text{D}_0$ excited state and the ground multiplet ($^7\text{F}_{0-4}$). Negligible emission from the organic part of the encapsulated species was detected, indicating that energy transfer from the ligand to the Eu^{3+} ion was quite efficient. Evaluation of the calculated radiative and non-radiative decay rates and comparison of the obtained Judd-Ofelt intensity parameters allowed for a strict correlation between the impregnation processes and the luminescence efficiencies of the prepared materials.

Keywords: mesoporous materials, lanthanide complex, photoluminescence.

1. INTRODUCTION

For many years, silica-gel has been used as a solid support in several areas [1-4]. In 1992, researchers at the Mobil Oil Company developed a new synthetic route for production of mesoporous materials known as the M41S family (MCM-41, MCM-48, and MCM-50). These materials possess large surface area and controlled pore volume, which are much desired characteristics for such materials [5-7]. The researchers used several ionic surfactants, mainly long-chain alkyltrimethylammonium halides, as structure-directing agents (SDAs). These SDAs produce ordered mesostructured composite during the condensation of the silica precursors under alkaline conditions [5,6]. The mesoporous materials are then obtained by complete removal of the surfactant either by extraction or by thermal treatment.

Since then, diverse mesoporous silica families, mostly SBA and MSU, have been prepared using many types of nonionic surfactants. The SBA silica family are synthesized by employing commercially available nonionic alkyl poly(ethylene oxide) (PEO) oligomeric surfactants and poly(alkylene oxide) block copolymers in acid media. The MSU family, on the other hand, can be produced by using the nonionic sorbitan monolaurate as structure-directing agent [8,9]. The synthesized silica matrix produced by co-condensation or post-grafting processes has been applied in many areas such as HPLC [10], adsorption of heavy metals [11] and catalysis [12], among others [13,14].

In addition, mesoporous silicas have been successfully applied in association with the remarkable properties of rare earth complexes, mainly those containing β -diketones and bipyridines.

In particular, the complexes containing trivalent lanthanides and β -diketonates have been extensively studied with regard to their alluring tribo-, electro-, and photoluminescent properties. Thus, these compounds have found important applications in several areas, such as optical devices (organic light emitting diodes, chelate lasers), Analytical Chemical (NMR shift reagents, gas chromatography stationary phases, luminescent sensors), and biological systems (MRI contrasts, fluoroimmunoassays) [15-17]. The great interest in applying β -diketonates in luminescent systems is due to their ability in overcoming the low molar absorptivity of the lanthanides (arising from their forbidden f-f transitions) by acting as light collectors. If the light absorption is followed by an efficient energy transfer process, the lanthanide emission quantum yields are pretty much improved by the so-called antenna effect [15,16,18]. Moreover, the incorporation of those coordination compounds into inorganic matrices is a very promising field, once their photophysical behavior can be modeled through interactions with the host and through the structure, besides conferring higher physico-chemical stabilities to the complex. Several papers on the use of lanthanide luminescent complexes incorporated into mesoporous silica matrix have been published [19,20]. However, despite the intense work in this field, the most effective synthetic methodology for impregnation of these complexes into the matrix remains undefined.

In this paper, we have synthesized the silica matrix by post-grafting process using polyoxyethylenesorbitan monolaurate (TWEEN 20), a nonionic surfactant. The silica surface was modified with the 3-aminopropyltriethoxysilane (APTS) sililant

agent. In order to determine the best methodology for impregnation of the [Eu(ttfa)₃] luminescent complex into the silica matrix, two routes were tested. First, the Eu³⁺ ions were incorporated into the silica matrix, and then the thenoyltrifluoroacetate (ttfa) organic ligand was added. In the second route, the luminescent complex was firstly synthesized

outside the inorganic matrix, followed by its addition to the mesoporous silica for impregnation. Furthermore, we were able to compare how the surfactant removal methodology (extraction or thermal treatment) can influence the luminescent properties of the produced silica matrices.

2. EXPERIMENTAL SECTION

2.1. Synthetic procedures.

2.1.1. Synthesis of the mesoporous silica. Two MSU-4 mesoporous silicas were prepared according to the two-step reaction process described by Boissière et al. [21]. Both syntheses followed the same experimental procedure except for the surfactant removal step, in which one of the silicas was purified by the extraction method in a soxhlet apparatus (MSU-4a), whereas the other was purified by calcinations (MSU-4b). All reagents including the nonionic surfactant (TWEEN 20, from Sigma), the silica source tetraethoxysilane (TEOS 98%, from Sigma-Aldrich), and sodium fluoride (NaF 99%, from Aldrich) were used without further purification.

In a typical synthesis, 2.456 g (2 mmol) TWEEN 20 were dissolved in 95 mL deionized water previously acidified at pH=2 with 1.0 mol L⁻¹ hydrochloric acid at room temperature, under moderate magnetic stirring. After full dissolution, 3.328 g (16 mmol) TEOS were added and the stirring was stopped. After a 12h aging at room temperature, this solution was heated at 35 °C and stirred. The final condensation step was induced by addition of 2.5 mL aqueous sodium fluoride (0.25 mol L⁻¹) to the solution, kept in a thermostated shaking bath under slow shaking for 3 days. Afterwards the final products (MSU-4a and MSU-4b) were filtered off and washed with water. Then, MSU-4a was washed in a soxhlet extractor with a 1:1 (v/v) water/ethanol solution (250 mL solution per 1 g of silica), while MSU-4b was calcined in air at 620 °C for 6 h, with a 6 h preliminary step at 200 °C (heating rate of 3 °C min⁻¹). The reaction yield was always higher than 95%.

2.1.2. Modified mesoporous silica. The MSU-4a mesoporous silica have been previously activated at 120 °C under vacuum and modified with 3-aminopropyltriethoxysilane (APTS 98%, from Sigma-Aldrich) by the post-grafting method, through addition of 0.93 mL (4.0 mmol) APTS per 1 g of silica, prepared by mixing APTS and mesoporous silica in 10.0 mL pure acetone. This mixture was stirred for 12 h under reflux and inert atmosphere. The solid product was filtered, washed with water and ethanol, and dried for 12 h at 120 °C under vacuum. This product were denoted MSU-4a-APTS.

2.1.3. Impregnation of Eu³⁺ ion into the silica matrices. As discussed above, two different methodologies of complex impregnation into the silica matrices were tested. The first method was used for impregnation of the MSU-4a, MSU-4b, and MSU-4a-APTS silica matrices. Firstly, a methanolic 0.10 mol L⁻¹ EuCl₃ stock solution was prepared through dissolution of the previously calcined (900 °C, 2 h) europium oxide (Eu₂O₃ 99.9%, from Aldrich) in concentrated hydrochloric acid; the pH of the solution was adjusted to ~5 through evaporation of excess acid and then methanol was added and successively evaporate to give up the

water molecules. Then, 2.5 mL (0.25 mmol) of this solution were mixed with 200 mg of the silica matrices at room temperature for 12 h, under constant stirring conditions. Next, 15 mL of a 0.05 mol L⁻¹ (0.75 mmol) sodium thenoyltrifluoroacetate methanolic solution (prepared through reaction of thenoyltrifluoroacetone – Httfa 99%, Sigma-Aldrich – with an equimolar amount of sodium hydroxide in methanol) was added to the mixture, which was kept under stirring for another 12 h. The obtained solid material was washed with water five times and dried at 100 °C for 12 h. These impregnated matrices will be denoted MSU-4a-Eu, MSU-4b-Eu and MSU-4a-APTS-Eu.

The second method was applied to impregnate the MSU-4a-APTS silica matrix only. It involved the preparation of the [Eu(ttfa)₃(H₂O)₂] complex, according to the procedure described by Charles et al. [22], before its impregnation into the mesoporous silica. For this, 17.5 mL of the [Eu(ttfa)₃(H₂O)₂] complex methanolic solution 0.015 mol L⁻¹ were then added to 200 mg of the MSU-4a-APTS solid, in order to impregnate the complex in the silica matrix; this system was kept under stirring for 12 h at room temperature. The obtained solid was washed with water five times and dried at 100°C for 12 h. This sample will be denoted MSU-4a-APTS-EuTTFA.

2.2. Characterization. The powders were characterized by scanning electron microscopy (SEM), transmission electron microscopy (TEM), X-ray diffractometry (XRD), N₂ adsorption/desorption, infrared spectroscopy (IR) and photoluminescent spectroscopy (PL). The X-ray diffractometer was a National Laboratory Synchrotron Light (LNLS-Campinas, Brazil) small angle X-Ray scattering (SAXS) line equipped with anode X-ray source ($\lambda = 1.488 \text{ \AA}$, functioning at 4 kW) and with a multilayer focusing ‘osmic’ monochromator giving high flux (108 photons s⁻¹) and punctual collimation. An ‘Image Plate’ 2D detector was employed. Fourier Transform Infrared (FT-IR) spectra were acquired (in KBr pellets) within the 4000-400 cm⁻¹ range with a 2 cm⁻¹ resolution, using a Nicolet Nexus 670 spectrometer. Scanning electron microscopy (SEM) micrographs were carried out at the LME/LNLS laboratory in Campinas, SP, using a Jeol JSM-5900 LV microscope operating at 20 kV.

Transmission electron microscopy (TEM) images were achieved on a Philips CM20 instrument operating at a 200 kV; the samples were ultrasonically dispersed in ethanol and dropped onto the carbon-coated copper grids prior to the measurements. Nitrogen absorption isotherms were measured at liquid-nitrogen temperature on a Micromeritics 2010 Sorptometer using standard continuous procedure. Surface areas were determined by the Brunnauer – Emmett – Teller (BET) method within a 0.05 – 0.02 relative pressure range. Pore size distributions were calculated

only for sizes higher than 2.5 nm from the desorption branch by a polynomial correlation between relative pressure and pore diameter, deduced from the Broekhoff and Boer (BdB) model [9,23]. To simplify comparison, we displayed the reduced adsorption curves (isotherms divided by the amount adsorbed at a relative pressure of 0.8) [24]. The excitation and emission spectra of the samples were recorded on a Horiba-Jobin Yvon SPEX

TRIAx Fluorolog 3 spectrofluorometer at room temperature, using a 450 W xenon arc lamp as light source and a Hamamatsu R928P photomultiplier for the detection. The luminescence lifetimes were obtained by coupling the phosphorimeter accessory (SPEX 1934D) to the spectrofluorometer, using a 150 W pulsed xenon lamp.

3. RESULTS SECTION

The SEM and TEM results for the MSU-4a silica (after surfactant removal) are displayed in Figure 1. The SEM (Figure 1a) micrographs reveal a spherical morphology, with a low degree of silica particle aggregation, which give a high surface area, as discussed later. The TEM image (Figure 1b) evidence that the particles contain domains of perfectly ordered structure. Nevertheless, because the TEM image shows the microscopic portion of the spherical particle, only a wider view of the structural and morphologic characteristics could not be observed. On the other hand, the overall view of the structure ordering of a macroscopic amount of the sample, obtained by means of SAXS, (Figure 2) indicates structural uniformity for the samples MSU-4a (Figure 2a), MSU-4b (Figure 2b) and MSU-4a-APTS (Figure 2c). The SAXS patterns also suggest where the nanostructure evolves from an amorphous state, with a long-range order described by a 3D wormhole structure [8]. For the MSU-4a, MSU-4b and MSU-4a-APTS samples, the observed d spacings are $d_{100} = 50 \text{ \AA}$, 47 \AA and 49 \AA , respectively, which agree with literature data [8].

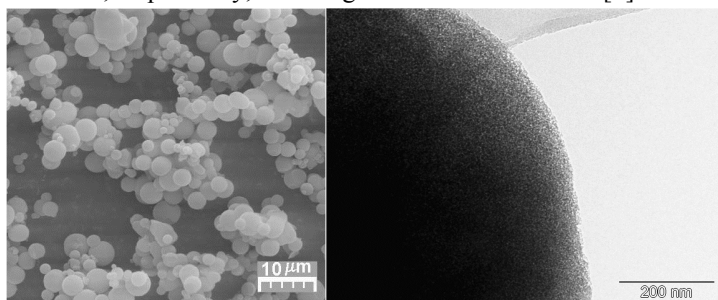


Figure 1. a) MSU-4a SEM micrograph at 1500x. b) MSU-4a TEM image.

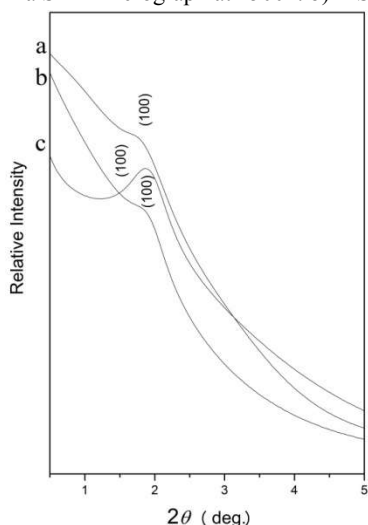


Figure 2. SAXS profiles of a) MSU-4a, b) MSU-4b and c) MSU-4a-APTS.

The nitrogen adsorption/desorption isotherms, Figure 3, are characteristics of mesoporous MTS-type materials [9]. Therefore, all samples exhibit substantial framework-confined mesopores. The isotherm of the samples does not exhibit any hysteresis, characteristic of pore necking, nor does the adsorption increase at high relative pressure, characteristic of a textural porosity.

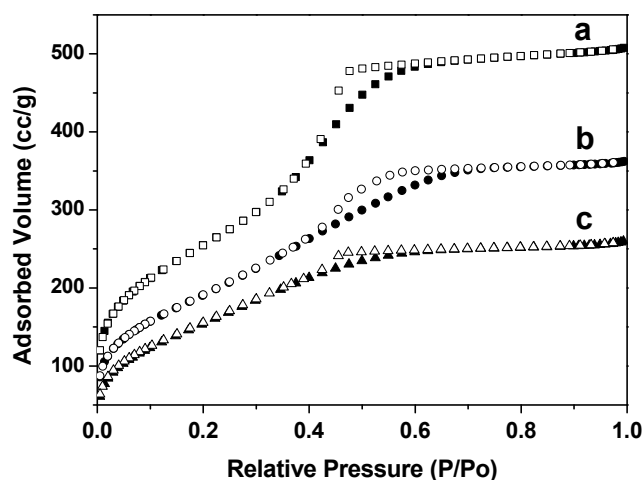


Figure 3. Reduced nitrogen adsorption (solid symbol)/desorption (open symbol) of mesoporous silica samples post-synthesis treated (a) washing water/ethanol solution, (b) calcination (c) chemical modification by APTS.

The pores size distributions for the samples are shown in Figure 4. The porosity of mesoporous silica samples decrease with type of post-synthesis treatment, thus, the pore size changed from 40 \AA to 34 \AA when the treatment changed of washing water/ethanol solution to chemical modification by APTS. Also, all samples presented pore size distributions, typical of mesoporous micelle-templated structures materials. The mesoporous silica samples exhibit a high surface area. The surface area is $930 \text{ m}^2 \text{ g}^{-1}$, $700 \text{ m}^2 \text{ g}^{-1}$ and $574 \text{ m}^2 \text{ g}^{-1}$ for mesoporous silica samples post-synthesis treated by washing water/ethanol solution, calcinations or chemical modification by APTS, respectively.

In addition, the wall thickness (inorganic palisade) of mesoporous silica, calculated by the difference of the d-spacing and the pore size, decreased when it changed post-synthesis treatment (washing water/ethanol solution to modification by APTS). This result is in agreement with XRD and pore size distribution, since the d-spacing and pore size increased with increasing chain length of surfactant molecules, Figure 4.

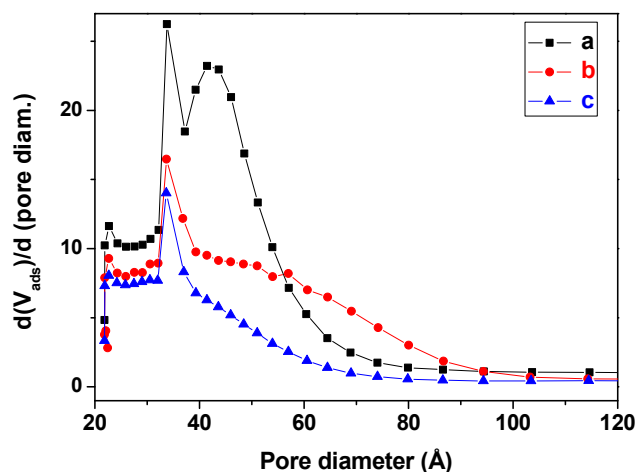


Figure 4. Evolution of pore diameter of calcined mesoporous silica samples post-synthesis treated (a) washing water/ethanol solution, (b) calcination (c) chemical modification by APTS.

The FT-IR spectra of a) MSU-4 with TWEEN 20, b) MSU-4a, c) MSU-4b, d) MSU-4a-APTS, e) MSU-4a-APTS-Eu and f) MSU-4a-APTS-EuTTFA are depicted in Figure 5. In figures 5a, 5b and 5c, the absence of the absorption bands at 2930 and 2850 cm^{-1} (ascribed to symmetric (ν_s) and anti-symmetric (ν_{as}) CH_2 stretching) and at 1740 cm^{-1} (associated with carbonyl ester organic function) give evidence of the removal of the TWEEN 20 surfactant molecules from the mesoporous silica. The amino-group vibrations can be detected in the spectrum of Figure 5d, where two new absorption bands, assigned ascribed to the N–H stretching modes of the primary amine, appear at 3100 cm^{-1} . The bands at 1558 cm^{-1} , attributed to the H–N–H bending (scissoring) vibrations, confirm the functionalization of the mesoporous silica. In Figures 5e and 5f, the displacement of the 1558 cm^{-1} absorption band to 1541 cm^{-1} confirms an effective interaction between the amino-group (MSU-4a-APTS) and the Eu^{3+} ions (MSU-4a-APTS-Eu and MSU-4a-APTS-EuTTFA).

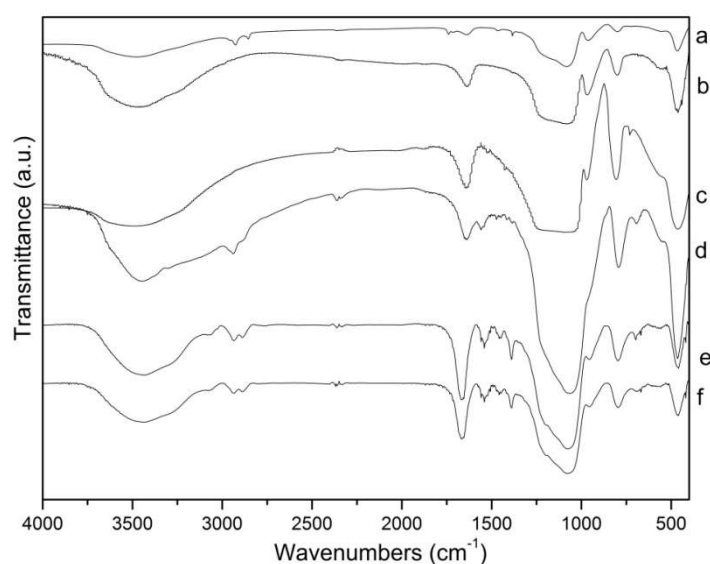


Figure 5. FT-IR spectra of a) MSU-4 with TWEEN 20, b) MSU-4a, c) MSU-4b, d) MSU-4a-APTS, e) MSU-4a-APTS-Eu and f) MSU-4a-APTS-EuTTFA.

Figure 6 presents the excitation spectra ($\lambda_{em}=612$ nm) of the $[\text{Eu}(\text{ttfa})_3(\text{H}_2\text{O})_2]$ free complex and of the Eu^{3+} -ttfa modified silica matrices (MSU-4a-Eu, MSU-4b-Eu, MSU-4a-APTS-Eu and MSU-4a-APTS-EuTTFA). All the spectra are dominated by the characteristic ttfa excitation, which attests for the coordination of

the β -diketonate to the lanthanide ion, thus resulting in efficient energy transfer to the Eu^{3+} ion. Regardless of the synthetic procedure, the incorporation of the complex into the silica matrices results in the sharpening of the ttfa excitation band, which is coherent with the occupation of sites with higher structural rigidities. Moreover, there is a hypsochromic shift (to lower wavelength) in the complex excitation maxima, which indicates that immobilization to the inorganic host leads to destabilization of the lowest unoccupied molecular orbitals (LUMO) of the complex. In other words, the interactions of the complex with the silica matrices reduce the excited state electron withdrawing ability of the ligands, thus leading to larger HOMO-LUMO separation [15].

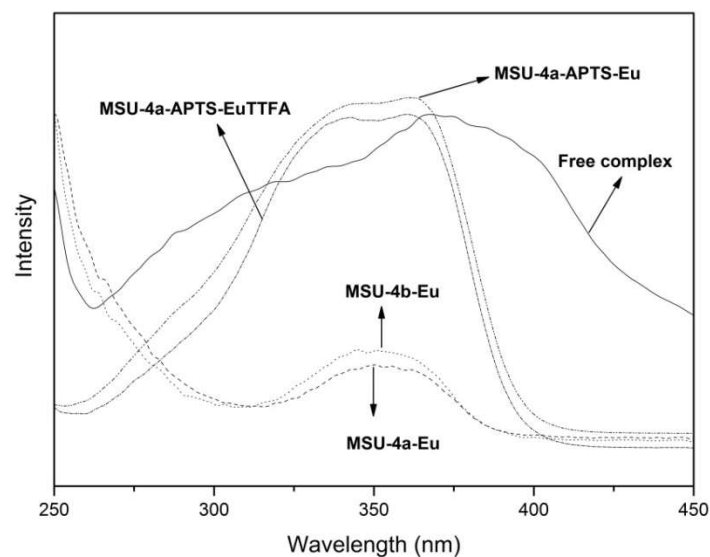


Figure 6. Excitation spectra ($\lambda_{em}=612$ nm) of the $[\text{Eu}(\text{ttfa})_3(\text{H}_2\text{O})_2]$ free complex, MSU-4a-Eu, MSU-4b-Eu, MSU-4a-APTS-Eu and MSU-4a-APTS-EuTTFA.

The emission spectra (Figures 7a and 7b) obtained under ligand excitation ($\lambda_{exc}=350$ nm) exhibit the characteristic Eu^{3+} $^5\text{D}_0 \rightarrow ^7\text{F}_J$ ($J = 0, 1, 2, 3, 4$) transitions with appreciable intensities, as a result of an efficient antenna effect.

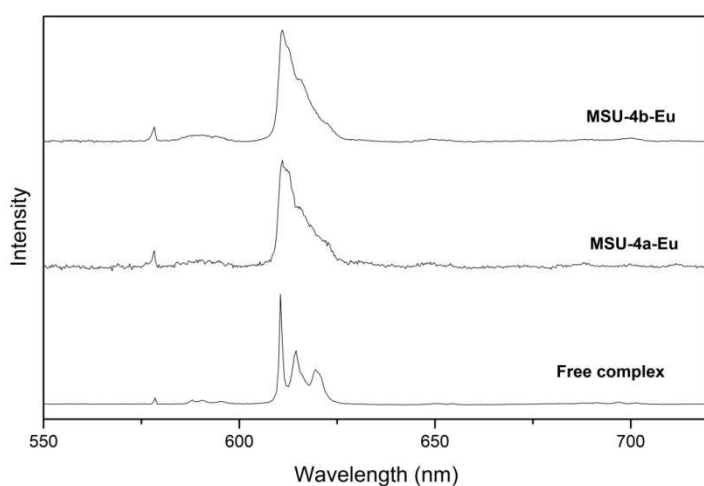


Figure 7a. Emission spectra ($\lambda_{exc}=350$ nm) of the $[\text{Eu}(\text{ttfa})_3(\text{H}_2\text{O})_2]$ free complex, MSU-4a-Eu and MSU-4b-Eu.

In all the cases, the same Eu^{3+} emission profile is observed, with dominance of the hypersensitive $^5\text{D}_0 \rightarrow ^7\text{F}_2$ transition at ~ 612 nm. This gives rise to an intense red luminescence output for all the samples, which is coherent with the occupation of low symmetry sites without inversion center (C_{2v} , C_2 , C_1 , C_s) [25].

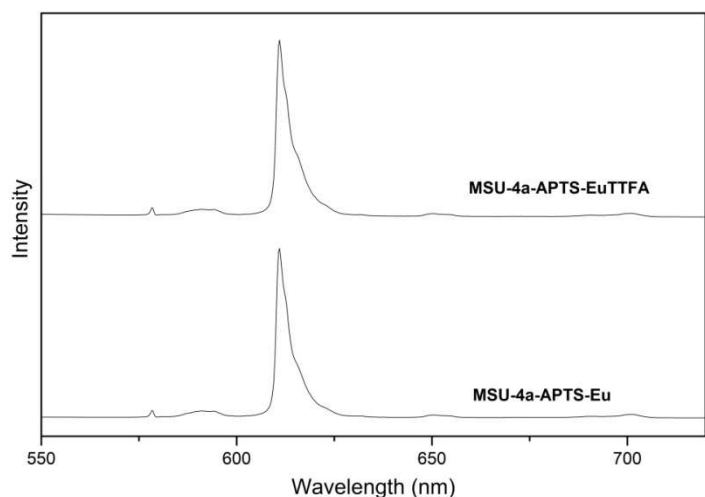


Figure 7b. Emission spectra ($\lambda_{\text{ex}}=350$ nm) of MSU-4a-APTS-Eu and MSU-4a-APTS-EuTTFA.

The experimental 5D_0 luminescence decay curves, of all the samples, obtained by monitoring the $^5D_0 \rightarrow ^7F_2$ transition under 350 nm excitation, exhibit a monoexponential profile, which is in agreement with a first order (or pseudo-first order) excited state kinetics [26]. This is related to the occurrence of coordination sites with very similar characteristics in each sample, so even with the incorporation into the silica, there is high homogeneity of Eu^{3+} coordination environments. The luminescence lifetimes (obtained by fitting the experimental decays for first order exponential functions) are presented in Table 1. In contrast with the occupation of sites with higher structural rigidity, the lifetimes of the MSU-4a-Eu and MSU-4b-Eu samples (0.20 and 0.23 ms) are expressively lower compared with that of the free complex (0.50 ms). This is a consequence of the occurrence of a high number of OH oscillators (silanol groups) in the inorganic hosts, leading to efficient non-radiative excited state deactivation and thus reduction in the lifetimes [27]. On the other hand, the aminopropyl-functionalized samples (MSU-4a-APTS-Eu and MSU-4a-APTS-EuTTFA) present higher luminescence lifetimes (0.82 and 0.67 ms), as a result of the exclusion of the surface OH groups, which contributes to multi-phonon deactivation. This also indicates the occurrence of a lower degree of interaction between the NH_2 groups and the Eu^{3+} ions compared with the silanol groups, once the NH oscillators also have high energies and can act as quenchers of the lanthanide luminescence [27].

For a deeper evaluation of the behavior of the Eu^{3+} ion, in the prepared systems, the radiative (A_{RAD}) and non-radiative (A_{NRAD}) decay rates were calculated from the emission spectra and luminescence lifetimes [18,28]. The effect of the silica matrices on the luminescence of the complex becomes clear from examination of the emission quantum efficiencies (ϕ , defined as the $A_{\text{RAD}}/(A_{\text{RAD}}+A_{\text{NRAD}})$ ratio). As discussed previously, in the MSU-4a-Eu and MSU-4b-Eu samples, the multi-phonon deactivation promoted by the large number of silanol groups leads to very high non-radiative decay rates. Thus, low ϕ values (14 and 17%) are found for these samples compared with the solid free complex (45%). Moreover, the occurrence of similar quantum efficiencies in the MSU-4a-Eu and MSU-4b-Eu solids also show that there are no significant alterations in the luminescence properties of the final materials with regard to the procedure employed for

surfactant elimination. In the functionalized samples, the results evidence that the solids have higher photoluminescence efficiencies compared with the free complex (58% and 71% for the MSU-4a-APTS-Eu and MSU-4a-APTS-EuTTFA samples, respectively), as a consequence of the occupation of more rigid environments with lower influence of vibrational quenching species. Furthermore, the incorporation of the complex to the silica matrices results in larger separation between the emitting centers, thus reducing the contribution of cross relaxation and other concentration quenching processes [17,25,26].

Table 1 also depicts the intensity ratios between the hypersensitive $^5D_0 \rightarrow ^7F_2$ transition and the magnetic dipole allowed $^5D_0 \rightarrow ^7F_1$ transition (I_{02}/I_{01}) for the prepared samples. This value is often taken as a qualitative indication of the centrosymmetric character of the Eu^{3+} coordination environment, once the $^5D_0 \rightarrow ^7F_2$ transition is intensified in the absence of inversion symmetry, while the $^5D_0 \rightarrow ^7F_1$ is practically independent of the site symmetry and has a constant emission decay rate ($A_{01} \approx 50 \text{ s}^{-1}$) [15,17,18]. The MSU-4a-Eu, MSU-4b-Eu and MSU-4a-APTS-Eu samples present lower I_{02}/I_{01} values compared with the free complex, which can be related to higher site symmetries, probably induced by strong intermolecular interactions with the host. In the MSU-4a-APTS-EuTTFA sample, these interactions are proven to be quite lower, once its I_{02}/I_{01} ratio is higher than those obtained for the other samples and close to that of the free complex. This is a consequence of the fact that during the MSU-4a-APTS-EuTTFA preparation the Eu^{3+} complex is already established before incorporation into the functionalized silica, so it displays very similar properties to those of the free complex after inclusion into the inorganic host.

The calculated Judd-Ofelt intensity parameters (Ω_2) [18,28], which contain information about the different mechanisms of 4f-4f transitions, are dependent on the lanthanide ion and on the occupied chemical environment only. So they also confirm the previous observations. In all the cases, the predominance of the Ω_2 parameter over Ω_4 ($\Omega_2 > \Omega_4$) indicates that the distribution of the ligand groups around the ions leads to predominance of the lower rank crystal field components over the higher rank ones, which can be correlated to sites of low centrosymmetric character for Eu^{3+} [16,18,28]. Moreover, the low value of the Ω_4 parameter suggests a low hypersensitive behavior for the $^5D_0 \rightarrow ^7F_4$ transition. The Ω_2 values achieved for the MSU-4a-Eu, MSU-4b-Eu and MSU-4a-APTS-Eu samples are lower than those obtained for the other preparations, which is a consequence of a relatively low hypersensitivity of the $^5D_0 \rightarrow ^7F_2$ transition in the former cases. This is related to the occupation of less polarizable chemical environments, as a result of a high degree of interaction of the lattice surface groups. On the other hand, the Ω_2 values for the MSU-4a-APTS-EuTTFA sample are comparable (and slightly higher) with those of the free complex. This confirms that the MSU-4a-APTS-EuTTFA synthetic procedure enables maintenance of the same coordination characteristics as those of the free complex, but also confers higher structural rigidity and reduces the energy transfer within the Eu^{3+} ions, thus yielding to a very efficient photoluminescent material.

Table 1. Luminescence lifetimes (5D_0 level), radiative and non-radiative decay rates, emission quantum efficiencies, ratio between integrated areas of the $^5D_0 \rightarrow ^7F_1$ and $^5D_0 \rightarrow ^7F_2$ transitions, and Judd-Ofel intensity parameters of the prepared samples

	τ (ms)	A_{RAD} (s^{-1})	A_{NRAD} (s^{-1})	ϕ (%)	I_{02}/I_{01}	Ω_2 ($10^{-20} cm^2$)	Ω_4 ($10^{-20} cm^2$)
Free complex	0.50	898	1102	45	16	27	2.3
MSU-4a-Eu	0.20	723	4277	14	12	20	2.9
MSU-4b-Eu	0.23	734	3614	17	12	21	2.7
MSU-4a-APTS-Eu	0.82	706	514	58	12	20	2.0
MSU-4a-APTS-EuTTFA	0.67	1062	431	71	19	33	2.2

(Luminescence lifetimes are accurate within 5%; the calculated parameters are accurate within 10%).

4. CONCLUSIONS

In summary, the $[Eu(tffa)_3(H_2O)_2]$ complex was successfully immobilized into the ordered MSU-4 mesoporous silica by modification with APTS using a post-grafting functionalization method, as confirmed by the FT-IR spectra. The SEM micrographs revealed a well defined spherical morphology, with low degree of silica particle aggregation while the TEM image evidenced that the particles contain domains of perfectly ordered structure. The SAXS profiles demonstrated a structural uniformity of the material for the mesoporous silica matrices and also indicated where the nanostructure evolves from an amorphous state, with a long-range order described by a 3D wormhole structure. The photoluminescence excitation spectra were dominated by the characteristic tffa excitation, which attests for the coordination of the β -diketone to the lanthanide ion, thus resulting in efficient energy transfer to the Eu^{3+} ion.

The emission spectra presented the characteristic Eu^{3+} $^5D_0 \rightarrow ^7F_J$ ($J = 0, 1, 2, 3, 4$) transitions with appreciable intensities, as a result of an efficient antenna effect. Moreover, the same Eu^{3+} emission profile was observed, with dominance of the hypersensitive $^5D_0 \rightarrow ^7F_2$ transition at ~ 612 nm, giving rise to an intense red luminescence output for the samples. The experimental 5D_0 luminescence decay curves of all the samples exhibited a monoexponential profile, which is in agreement with the occupation of quite similar symmetry sites in each solid. The effect of the silica matrices on the luminescence of the complex becomes clear with the evaluation of the emission quantum efficiencies and f-f intensity parameters. In conclusion, the developed procedures have shown to be quite appropriate impregnation methodologies, which give rise to wide applications with better efficiency in the optical or electronic areas.

5. REFERENCES

- [1] Leyden D. E., Luttrell G. H., Sloan A. E., de Angelis N. J., Characterization and Application of Silylated Substrates for the Preconcentration of Cations, *Analytica Chimica Acta*, 84, 97-108, **1976**.
- [2] Gimpel M., Unger K., Monomeric vs. polymeric bonded iminodiacetate silica supports in high-performance ligand-exchange chromatography, *Chromatographia*, 17, 200-204, **1983**.
- [3] Capka M., Heftlejls J., Hydrosilylation catalysed by transition metal complexes coordinately bound to inorganic supports, *Collect. Czech. Chem. Commun.* 39, 154-166, **1974**.
- [4] Martines M. A. U., Davolos M. R., Jafelicci M. J., Souza D. F., Nunes L. A. O., Cr^{3+} and Cr^{4+} luminescence in glass ceramic silica, *Journal of Luminescence*, 128, 1787-1790, **2008**.
- [5] Kresge C. T., Leonowicz M. E., Roth W. J., Vartuli J. C., Beck J. S., Ordered mesoporous molecular sieves synthesized by a liquid-crystal template mechanism, *Nature*, 359, 710-712, **1992**.
- [6] Beck J. S., Vartuli J. C., Roth W. J., Leonowicz M. E., Kresge C. T., Schmitt K. D., Chu C. T. W., Olson D. H., Sheppard E. W., McCullen S. B., Higgins J. B., Schlenker J. L., A new family of mesoporous molecular sieves prepared with liquid crystal templates, *Journal of the American Chemical Society*, 114, 10834-10843, **1992**.
- [7] Monnier A., Schuth F., Huo Q., Kumar D., Margolese D., Maxwell R. S., Stucky G. D., Krishnamurthy M., Petroff P., Firouzi A., Janicke M., Chmelka B. F., Cooperative formation of inorganic-organic interfaces in the synthesis of silicate mesostructures, *Science*, 261, 1299-1303, **1993**.
- [8] Zhao D., Huo Q., Feng J., Chmelka B. F., Stucky G. D., Nonionic Triblock and Star Diblock Copolymer and Oligomeric Surfactant Syntheses of Highly Ordered, Hydrothermally Stable, Mesoporous Silica Structures, *Journal of the American Chemical Society*, 120, 6024-6036, **1998**.
- [9] Prouzet E., Cot F., Nabias G., Larbot A., Kooyman P., Pinnavaia T. J., Assembly of mesoporous silica molecular sieves based on nonionic ethoxylated sorbitan esters as structure directors, *Chemistry of Materials*, 11, 1498-150, **1999**.
- [10] Martines M. A. U., Yeong E., Persin M., Larbot A., Voorthout W. F., Kübel C. K. U., Kooyman P., Prouzet E. C. R., Hexagonal mesoporous silica nanoparticles with large pores and a hierarchical porosity tested for HPLC, *Chimie*, 8, 627-634, **2005**.
- [11] Jorgetto, A. O., Pereira S. P., Silva R. I. V., Saeki M. J., Martines, M. A. U., Pedrosa V. A., Castro G. R., Application of mesoporous SBA-15 silica functionalized with 4-amino-2-mercaptopyrimidine for the adsorption of Cu(II), Zn(II), Cd(II), Ni(II), and Pb(II) from water, *Acta Chimica Slovenica*, 62, 111-121, **2015**.
- [12] de Oliveira E., Néri C. R., Ribeiro A. O., Garcia V. S., Costa L. L., Moura A. O., Prado A. G. S., Serra O. A., Iamamoto Y., Hexagonal mesoporous silica modified with copper phthalocyanine as a photocatalyst for pesticide 2,4-dichlorophenoxyacetic acid degradation, *Journal of Colloid and Interface Science*, 323, 98-104, **2008**.
- [13] Hoffmann F., Cornelius M., Morell J., Fröba M., Silica-based mesoporous organic-inorganic hybrid materials, *Angewandte Chemie International Edition*, 45, 3216-3251, **2006**.
- [14] Rocha L. A., Caiut J. M. A., Messaddeq Y., Ribeiro S. J. L., Martines M. A. U., Freiria J. C., Dexpert-Ghys J., Verelst M., Non-leachable highly luminescent ordered mesoporous SiO₂ spherical particles, *Nanotechnology*, 21, 155603-155608, **2010**.

- [15] Binnemans K., in: Gschneidner K. A. J., Bünzli J. C. G., Pecharsky V.K., Handbook on the Physics and Chemistry of the Rare Earths, Elsevier, Amsterdam, **2005**.
- [16] Brito H. F., Malta O. L., Felinto M. C. F. C., Teotônio E. E. S. in: J. Zabicky, The Chemistry of Metal Enolates Vol. 1, John Wiley & Sons Ltd., West Sussex, **2009**.
- [17] Mendes L. S., Saska S., Martines M. A. U., Marchette R., Nanostructured materials based on mesoporous silica and mesoporous silica/apatite as osteogenic growth peptide carriers, *Materials Science and Engineering C*, 33, 4427-4434, **2013**.
- [18] Lechevallier S., Jorge J., Silveira R. M., Ratel-Ramond N., Neumeyer D., Menu M. J., Gresseir M., Marçal A. L., Rocha L. A., Martines M. A. U., Magdeleine E., Dexpert-Ghys J., Verelst M., Luminescence properties of mesoporous silica nanoparticles encapsulating different europium complexes: application for biolabelling, *Journal of Nanomaterials*, v. 2013, Article ID 918369, 11 pages, **2013**.
- [19] de Oliveira E., Néri C. R., Serra O. A., Prado A. G. S., Antenna effect in highly luminescent Eu³⁺ anchored in hexagonal mesoporous silica, *Chemistry of Materials*, 19, 5437-5442, **2007**.
- [20] Sigoli F. A., Brito H. F., Jafelicci M. J., Davolos M. R., Luminescence of Eu (III) β -diketone complex supported on functionalized macroporous silica matrix *International Journal of Inorganic Chemistry*, 3, 755-762, **2001**.
- [21] Boissière C., Martines M. A. U., Tokumoto M., Larbot A., Prouzet E., Mechanisms of Pore Size Control in MSU-X Mesoporous Silica, *Chemistry of Materials*, 15, 509-515, **2003**.
- [22] Charles R. G., Ohlmann R.C., Europium thenoyltrifluoroacetate, preparation and fluorescence properties, *Journal of Inorganic and Nuclear Chemistry*, 27, 255-259, **1968**.
- [23] Broekhoff, J. C. P., de Boer, J. H., Studies on pore systems in catalysts. XIII. Pore distributions from the desorption branch of a nitrogen sorption isotherms in the case of cylindrical pores. B. Applications, *Journal of Catalysis*, 10, 377-390, **1968**.
- [24] Ryoo R., Ko C. K., Kruk M., Antochshuk V., Jaroniec M., Block-copolymer-templated ordered mesoporous silica: array of uniform mesopores or mesopore-micropore network? *The Journal of Physical Chemistry B*, 104, 11465-11471, **2000**.
- [25] Bünzli J. C. G. in: Bünzli J. C. G., Choppin G. R., Lanthanide Probes in Life, Chemical and Earth Sciences, Elsevier, Amsterdam, **1989**.
- [26] Blasse G., Grabmaier B. C., Luminescent Materials, Springer, Berlin, **1994**.
- [27] Supkowski R. M., Horrocks W. D. W. J., On the determination of the number of water molecules, q, coordinated to europium(III) ions in solution from luminescence decay lifetimes, *Inorganica Chimica Acta*, 340, 44-48, **2002**.
- [28] Kodaira C. A., Brito H. F., Malta O. L., Serra O. A., Luminescence and energy transfer of the europium (III) tungstate obtained via the Pechini method, *Journal of Luminescence*, 101, 11-21, **2001**.

6. ACKNOWLEDGEMENTS

The authors gratefully acknowledge CNPq, CAPES, CNPq/RENAMI/inct-INAMI, FAPESP and FUNDECT-MS for its financial support of this work, and the Brazilian Synchrotron Light Laboratory – LNLS for the SAXS and SEM (LME/LNLS) measurements.

© 2016 by the authors. This article is an open access article distributed under the terms and conditions of the Creative Commons Attribution license (<http://creativecommons.org/licenses/by/4.0/>).